Vietnam Journal of Mechanics, VAST, Vol. 44, No. 2 (2022), pp. 153 – 168
DOI: https://doi.org/10.15625/0866-7136/16846

AN APPROACH ON THE VIBRO-ACOUSTIC PROPERTIES OF COMPOSITE SANDWICH PLATES WITH FOAM CORE

Tran Ich Thinh[1,*]
[1]*Hanoi University of Science and Technology, Hanoi, Vietnam*
[*]E-mail: thinh.tranich@hust.edu.vn

Received: 27 December 2021 / Published online: 29 June 2022

Abstract. In this paper, an approach is proposed and presented to tackle the vibro-acoustic properties of finite clamped composite sandwich plates with foam core. Composite sandwich plates are treated as being orthotropic and the apparent bending stiffnesses are calculated for the two principal directions. The apparent bending stiffnesses of composite sandwich plate are estimated by finite element calculation on beam elements cut from the considered composite sandwich plates. The sound transmission loss of clamped composite sandwich plates is predicted using orthotropic Kirchhoff's plate theory, together with the obtained bending stiffnesses in two principal directions. Several sound transmission loss measurements were conducted in the laboratory on fiberglass/polyester composite sandwich plates with polyurethane foam core. The predicted sound transmission loss is compared with measured data and the agreement is reasonable.

Keywords: vibroacoustic properties, composite sandwich plate, foam core, sound transmission loss, apparent bending stiffness.

1. INTRODUCTION

The composite sandwich plate with a foam core is widely used in many industries, including aircraft, building, motor vehicle and ships because of the advantages like high strength, light weight, low cost and good sound insulation. A very important vibro-acoustic index used to measure the potential of sandwich plates to absorb sounds transmitted through them is the sound transmission loss (STL). This is the ratio of the sound power incident on the incident plate to the sound power transmitted by the radiating plate. The STL of sandwich structures has been the subject of many studies [1–5]. Especially, Sahu et al. [6] investigated the active control of sound transmission through sandwich plate with a soft core using volume velocity cancellation. D'Alessandro et al. [7]

reviewed the most significant works in literature of the acoustic behavior of sandwich panels including theoretical and experimental methods. In [8], by applying modal expansion method, Shen et al. proposed a theoretical model to predict the STL of a simply supported sandwich plate with corrugated core. Naify et al. [9] presented transfer matrix method and experiment to determine the transmission loss of honeycomb sandwich plate with attached gas layers. Based on Mindlin's plate theory [10], Wang et al. [11] derived the governing equation of bending vibration for unbounded orthotropic sandwich panels with orthotropic composite skins and honeycomb core, and used the impedance method, these authors also obtained the expression for transmission coefficient. Zhou et al. [12] studied and optimized the sound transmission loss through a sandwich panel with poroelastic core layer. Nilsson [13] proposed a method to determine the dynamic properties of sandwich panels by some simple measurements on sandwich beams.

In [14], Qu et al. used Finite element method to model the vibroacoustic emission of composite sandwich structures. An improved method-the wave finite element method described by Mace and Mancony [15], Droz et al. [16] and Chronopoulos et al. [17], is a numerical model reduction method which permits the modelling of each cell element rather than modelling the complete structure. The method entails the combination of both the finite element and the periodicity of the structure with the advantage of low computational cost. Recently, Yang et al. [18,19] has applied this model to predict the STL of multi-layered plates with fluid layers. In short, to describe the vibration-acoustic response and calculate the STL of composite sandwich plates, one can apply various methods, mathematical models and theories such as: Analytical method, Numerical method and/or Experimental method; Kirchhoff's plate theory or Mindlin's plate theory for face sheets sandwich plate and Biot's theory for poroelastic core layer.

In this paper, fiberglass/polyester composite sandwich plates with a foam core, PU (Polyurethane), are treated as being orthotropic and the apparent bending stiffness is calculated for the two principal directions. The apparent bending stiffness of composite sandwich plate is estimated by finite element calculation on sandwich beams cut from the considered composite sandwich plate. Using standard orthotropic Kirchhoff thin plate theory, together with the obtained bending stiffness in two directions, the sound transmission loss of finite clamped composite sandwich plates is predicted with modal expansion method. Some experiments to measure the sound transmission loss were carried out in the laboratory on considered composite sandwich plates. The predicted STL is also compared with experimental results.

2. THEORETICAL FORMULATION

2.1. Plate geometry and assumptions

Suppose there is a finite, rectangular composite sandwich plate clamped on four edges, as shown in Fig. 1. The sandwich plate for this study refers to a structure consisting of two thin laminated composite sheets bonded to a polyurethane foam core. The sandwich plate has length a along x-direction, width b along y-direction and thickness along z-direction.

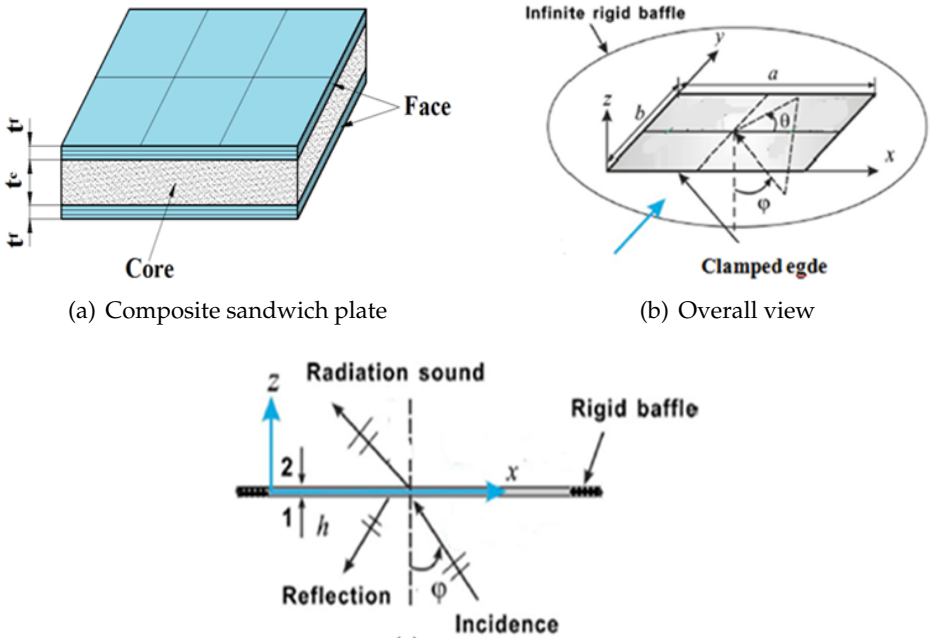

(a) Composite sandwich plate (b) Overall view

(c) Side view from the direction of arrow in (b)

Fig. 1. Schematic of sound transmission across a clamped rectangular composite sandwich plate

Obviously, the plate divides the spatial region into two modes: the incident field ($z < 0$) and the transmitted field ($z > 0$). An oblique plane sound wave varying harmonically in time is incident on the bottom side of the plate, with elevation angle φ and azimuth angle θ, Fig. 1(b). The plate vibration induced by the positive-going wave and the negative-going wave (including the reflected wave and the radiating wave) in the incident acoustic field, and the positive-going wave in the transmitted field. The pressure changes caused by this disturbance will in turn significantly influence the plate vibration, resulting the so-called composite laminated plate coupling. In the present study, it is assumed that the plate deforms out of plane (in the z-direction), positive upward.

2.2. Composite sandwich plate dynamics

In most applications, and for simplicity, the composite sandwich plate can be regarded as an orthotropic single plate. The dynamical displacement of an orthotropic symmetric composite plate in the air on both sides and subjected to uniform, plane sound wave varying harmonically can be described by [11,13]

$$D_x \frac{\partial^4 w(x,y;t)}{\partial x^4} + 2\sqrt{D_x D_y}\frac{\partial^4 w(x,y;t)}{\partial x^2 \partial y^2} + D_y \frac{\partial^4 w(x,y;t)}{\partial y^4} + m^* \frac{\partial^2 w(x,y;t)}{\partial^2 t} - j\omega\rho_0 \left[\Phi_1(x,y,z;t) - \Phi_2(x,y,z;t)\right] = 0, \tag{1}$$

where w is the normal displacement of the plate, D_x and D_y are the apparent bending stiffnesses in x and y directions, respectively, m^* is the surface density of the plate, ρ_0 is the air density, ω is the angular frequency of the incident sound and $\Phi_i\ (i = 1,2)$ denote the velocity potentials for the acoustic fields in the proximity of the plate, corresponding to the sound incidence and the structure radiating field, respectively.

The displacement of the composite sandwich plate induced by the incident sound can be expressed as

$$w(x,y;t) = w_0 e^{-j(k_x x + k_y y - \omega t)}. \tag{2}$$

The acoustic velocity potential in the incident field (Fig. 1) is defined by [8]

$$\Phi_1(x,y,z;t) = I e^{-j(k_x x + k_y y + k_z z - \omega t)} + \beta e^{-j(k_x x + k_y y - k_z z - \omega t)}, \tag{3}$$

where I and β are the amplitudes of the incident and the reflected waves, respectively. Similarly, in the transmitting field adjacent to the radiating upper plate, there exist no reflected waves, and therefore the velocity potential in the transmitting waves, given as:

$$\Phi_2(x,y,z;t) = \varepsilon\, e^{-j(k_x x + k_y y + k_z z - \omega t)}, \tag{4}$$

where ε is the amplitude of the transmitting wave. These wave numbers are determined by the elevation angle φ and azimuth angle θ of the incident sound wave as

$$k_x = k_0 \sin\varphi\cos\theta; \quad k_y = k_0 \sin\varphi \sin\theta; \quad k_z = k_0 \cos\varphi, \tag{5}$$

where $k_0 = \omega/c_0$ is the acoustic wave number in air a c_0 is the acoustic speed in the air.

With the plate fully clamped on four edges, the boundary conditions can be expressed as

$$x = 0, a, \quad w = 0, \quad \frac{\partial w}{\partial x} = 0; \quad y = 0, b, \quad w = 0, \quad \frac{\partial w}{\partial y} = 0. \tag{6}$$

At the air-plate interface, the normal velocity is continuous, yielding the corresponding velocity compatibility condition equations

$$z=0,\quad \frac{\partial \Phi_1}{\partial z}=\frac{\partial \Phi_2}{\partial z}=j\omega w;\quad z=h,\quad \frac{\partial \Phi_1}{\partial z}=\frac{\partial \Phi_2}{\partial z}=j\omega w. \tag{7}$$

By using the orthogonal plate eigenfunctions and the generalized coordinates, the dynamical displacement of the composite sandwich plate can be rewritten as

$$w\left(x,y;t\right)=\sum_{m=1}^{\infty}\sum_{n=1}^{\infty}\varphi_{mn}\left(x,y\right)q_{mn}\left(t\right)=\sum_{m=1}^{\infty}\sum_{n=1}^{\infty}\left(1-\cos\frac{2m\pi x}{a}\right)\left(1-\cos\frac{2n\pi x}{b}\right)\alpha_{mn}e^{j\omega t}, \tag{8}$$

where $q_{mn}(t)=\alpha_{mn}e^{j\omega t}$. Similarly, the acoustical velocity potentials of Eqs. (3) and (4) are expressed by [8]

$$\Phi_1(x,y,z;t)=\sum_{m=1}^{\infty}\sum_{n=1}^{\infty}I_{mn}\varphi_{mn}e^{-j(k_z z-\omega t)}+\sum_{m=1}^{\infty}\sum_{n=1}^{\infty}\beta_{mn}\varphi_{mn}e^{-j(-k_z z-\omega t)}, \tag{9}$$

$$\Phi_2(x,y,z;t)=\sum_{m=1}^{\infty}\sum_{n=1}^{\infty}\varepsilon_{mn}\varphi_{mn}e^{-j(k_z z-\omega t)}. \tag{10}$$

From the general forms of Eqs. (2)–(4) and the generalized forms of Eqs. (8)–(10), by utilizing the Cosine Fourier transform, one can obtained the following expression

$$\chi_{mn}=\frac{4}{ab}\int_0^b\int_0^a\chi e^{-j(k_x x+k_y y)}\cos\frac{2m\pi x}{a}\cos\frac{2n\pi x}{b}\mathrm{d}x\mathrm{d}y, \tag{11}$$

where the symbol χ can be referred to any of the coefficients I,β and ε.

2.3. Displacement continuity condition at air-plate interfaces

Suppose ξ_1 and ξ_2 are the acoustic particle displacements in the incident and transmitted air medium, respectively. The air particle displacement and the acoustic pressure are related by the air momentum equation, as [20]

$$\frac{\partial^2}{\partial t^2}\xi_1=-\left.\frac{1}{\rho_0}\frac{\partial p_1}{\partial z}\right|_{z=0},\quad \frac{\partial^2}{\partial t^2}\xi_2=-\left.\frac{1}{\rho_0}\frac{\partial p_2}{\partial z}\right|_{z=0}, \tag{12}$$

where, the acoustic pressure can be expressed by the acoustical velocity potentials through Bernoulli's equation, as [8]

$$p_i=\rho_0\left[\frac{\partial \Phi_i}{\partial t}\right],\ (i=1,2). \tag{13}$$

The displacements of the air particle adjacent to the plate can be expressed as

$$\xi_1=\xi_{10}e^{-j(k_x x+k_y y-\omega t)},\quad \xi_2=\xi_{20}e^{-j(k_x x+k_y y-\omega t)}. \tag{14}$$

Substituting (13), (14) into (12), and applying the acoustical velocity potentials of (9) and (10), one can obtain

$$\begin{aligned}\xi_{10} &= \left(\sum_{m,n=1}^{\infty} I_{mn}\varphi_{mn} - \sum_{m,n=1}^{\infty} \beta_{mn}\varphi_{mn}\right)\frac{k_z}{\omega}e^{j\left(k_x x+k_y y\right)},\\ \xi_{20} &= \sum_{m,n=1}^{\infty} \varepsilon_{mn}\varphi_{mn}\frac{k_z}{\omega}e^{j\left(k_x x+k_y y\right)}.\end{aligned} \tag{15}$$

According to the continuity condition, the displacement of the air particles at the surface adjacent to the plate must be equal to the displacement of the particles of attached plate surface, thus

$$\xi_{10} = w_0, \quad \xi_{20} = w_0. \tag{16}$$

From (11), we obtain the following relation between coefficients I_{mn} and I_0 (initial amplitude of incident wave)

$$I_{mn} = \frac{4I_0 abk_x^2 k_y^2\left(1-e^{-jk_x a}\right)\left(1-e^{-jk_y b}\right)}{\left(4m^2\pi^2 - k_x^2 a^2\right)\left(4n^2\pi^2 - k_y^2 b^2\right)}, \tag{17}$$

and from (2), (14), (15) and (16), one can express the coefficients in the acoustical velocity potentials by the plate displacement coefficients, as

$$\beta_{mn} = I_{mn} - \frac{\omega}{k_z}\alpha_{mn}, \quad \varepsilon_{mn} = \frac{\omega}{k_z}\alpha_{mn}. \tag{18}$$

Substituting (9) and (10) into (1) and applying the orthogonality of the modal functions, one gets

$$\ddot{q}_{mn} + \omega_{mn}^2 q_{mn}(t) - \frac{j\omega\rho_0}{m^*}\left[I_{mn}e^{-j(k_z z-\omega t)} + \beta_{mn}e^{-j(-k_z z-\omega t)} - \varepsilon_{mn}e^{-j(k_z z-\omega t)}\right] = 0, \tag{19}$$

where $m^* = 2t_s\rho_s + t_c\rho_c$ and the natural frequencies of clamped orthotropic rectangular composite sandwich plate are determined by

$$\omega_{mn}^2 = \frac{\iint\limits_A \left(D_x\frac{\partial^4\varphi_{mn}}{\partial^4 x} + 2\sqrt{D_x D_y}\frac{\partial^4\varphi_{mn}}{\partial^2 x\partial^2 y} + D_y\frac{\partial^4\varphi_{mn}}{\partial^4 y}\right)\varphi_{mn}\mathrm{d}A}{m^*\iint\limits_A \varphi_{mn}\cdot\varphi_{mn}\mathrm{d}A}. \tag{20}$$

Therefore, the coefficient α_{mn} is defined from (19) by:

$$\alpha_{mn} = \frac{2j\omega\rho_0 I_{mn}}{m^*}\left[\omega_{mn}^2 - \omega^2 + 2\frac{j\omega^2\rho_0}{mk_z}\right]^{-1}. \tag{21}$$

Once the plate displacement coefficients α_{mn} are known, the acoustical velocity potentials will be known and given by

$$\begin{aligned}\Phi_1(x,y,0) &= 2Ie^{-j\left(k_x x+k_y y\right)} - \sum_{m=1}^{\infty}\sum_{n=1}^{\infty}\frac{\omega}{k_z}\alpha_{mn}\varphi_{mn}(x,y),\\ \Phi_2(x,y,0) &= \frac{\omega}{k_z}\sum_{m=1}^{\infty}\sum_{n=1}^{\infty}\alpha_{mn}\varphi_{mn}(x,y).\end{aligned} \tag{22}$$

3. DEFINITION OF SOUND TRANSMISSION LOSS

The power of incident sound is defined as [20]

$$\Pi_1 = \frac{1}{2}Re\iint_A p_1 v_1^* \mathrm{d}A, \tag{23}$$

where $v_1^* = p_1/\left(\rho_0 c_0\right)$ is the local acoustic velocity, and p_1 is the sound pressure in the incident field,

$$p_1 = j\rho_0\omega\,\Phi_1\left(x,y,0\right) = j\rho_0\omega\left[2Ie^{-j\left(k_x x+k_y y\right)} - \sum_{m=1}^{\infty}\sum_{n=1}^{\infty}\frac{\omega}{k_z}\alpha_{mn}\varphi_{mn}(x,y)\right]. \tag{24}$$

Substitution p_1 and v_1^* into (23) yields

$$\begin{aligned}\Pi_1 = \frac{\rho_0\omega^2}{2c_0}\Bigg|4I^2\iint_A e^{-2j\left(k_x x+k_y y\right)}\mathrm{d}A - 4I\frac{\omega}{k_z}\sum_{m,n=1}^{\infty}\alpha_{mn}\iint_A e^{-j\left(k_x x+k_y y\right)}\varphi_{mn}\mathrm{d}A\\ +\frac{\omega^2}{k_z^2}\sum_{m,n=1}^{\infty}\sum_{k,l}^{\infty}\alpha_{mn}\alpha_{kl}\iint_A \varphi_{mn}(x,y)\varphi_{kl}(x,y)\mathrm{d}A\Bigg|.\end{aligned}$$

The transmitted sound power can be defined as

$$\Pi_2 = \frac{1}{2}Re\iint_A p_2 v_2^*\mathrm{d}A = \frac{\rho_0\omega^4}{2c_0k_z^2}\left|\sum_{m,n=1}^{\infty}\sum_{k,l=1}^{\infty}\alpha_{mn}\alpha_{kl}\iint_A \varphi_{mn}(x,y)\varphi_{kl}(x,y)\mathrm{d}A\right|, \tag{25}$$

where $v_2^* = p_2/\left(\rho_0 c_0\right)$ is the local acoustic velocity and p_2 is the sound pressure in the transmitted field,

$$p_2 = j\rho_0\omega\,\Phi_2\left(x,y,0\right) = j\rho_0\frac{\omega^2}{k_z}\sum_{m=1}^{\infty}\sum_{n=1}^{\infty}\alpha_{mn}\varphi_{mn}(x,y). \tag{26}$$

Finally, the power transmission coefficient can be obtained as

$$\tau_0\left(\theta,\varphi,f\right) = \frac{\Pi_2}{\Pi_1}. \tag{27}$$

The diffuse field sound transmission coefficient over all angles of incidence φ and θ is calculated by [8]

$$\tau_d = \frac{\int_0^{2\pi}\int_0^{\theta_L} \tau_0(\varphi,\theta,f)\sin\varphi\cos\varphi \mathrm{d}\varphi\mathrm{d}\theta}{\int_0^{2\pi}\int_0^{\theta_L} \sin\varphi\cos\varphi\mathrm{d}\varphi\mathrm{d}\theta}. \tag{28}$$

The integral (28) has been evaluated numerically by using Simpson's 1/3 rule with 15°-angular increments in φ and θ. θ_L is the *limiting angle of incidence* and is taken as 78° for field-incidence calculations.

Then the sound transmission loss across the composite sandwich plate is defined by:

$$STL = 10\log_{10}\left(\frac{1}{\tau_d}\right). \tag{29}$$

4. DETERMINATION OF APPARENT BENDING STIFFNESS

For homogeneous plates, the bending stiffness is frequency independent; however, for sandwich plates, the bending stiffness becomes frequency dependent. According to Nilsson's model [13], as an approximation, the bending stiffness of a sandwich plate can be defined as that of a simple homogeneous beam having the same dynamic properties as the plate at certain frequencies. In general, the apparent bending stiffnesses of sandwich plates can be determined by measuring the natural frequencies of beams cut out of the structures. But in this study, the apparent bending stiffnesses of the studied composite sandwich plates were inferred basing on the natural frequencies calculated by the finite element method for the aforementioned beams. That is also the key step of this work.

The sandwich plates studied here are manufactured with polyurethane foam core, as shown in Fig. 2. Eight different composite sandwich plates are investigated here, and their properties are measured and shown in Table 1. The sheets are made of glass fiber/polyester symmetric composites with configuration $[0^\circ/90^\circ/0^\circ]_s$ for plate A, C, E, G and $[0^\circ/90^\circ/0^\circ/90^\circ]_s$ for plate F; H, I, K; t_s and t_c denotes the thickness of skin and core respectively.

Beam A0 and A90 were cut from plate A along the 0° (or x) and 90° (or y) directions respectively. The same operations are done to the other plates. The sizes of beams A0, C0, E0, F0, G0, H0, I0 and K0 are 1200 mm × 50 mm; the sizes of beams A90 and C90, E90, F90, G90, H90, I90 and K90 are 1100 mm × 45 mm.

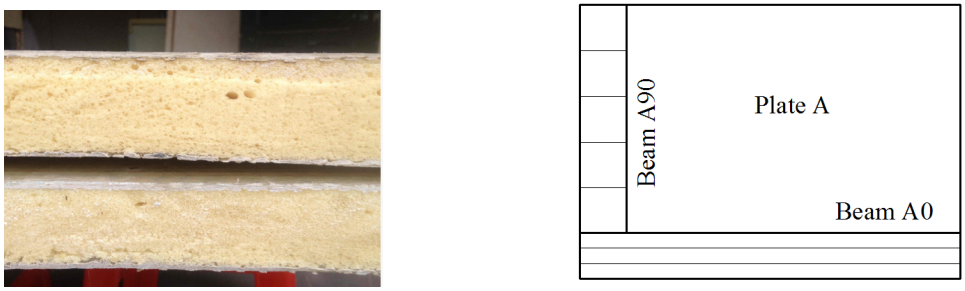

Fig. 2. Composite sandwich plate and beams A0, A90

Table 1. Properties of composite sandwich plates tested

Plate	$a \times b$ (m)	Thickness $t_s/t_c/t_s$ ($\times 10^{-3}$ m)	Skin density ρ_s (kg/m^3)	Core density ρ_c (kg/m^3)	E_1 (GPa)	E_2 (GPa)	G_{12} (GPa)	v_{12}	E_c (GPa)	v_c
A	1.2 × 1.2	2.53/30/2.53	1600	46.880	10.580	2.640	1.020	0.17	0.0570	0.25
C	1.2 × 1.2	2.53/30/2.53	1600	57.870	10.580	2.640	1.020	0.17	0.0580	0.25
E	1.2 × 1.2	2.53/30/2.53	1600	79.860	10.580	2.640	1.020	0.17	0.0585	0.25
F	1.2 × 1.2	3.37/30/3.37	1600	79.860	10.580	2.640	1.020	0.17	0.0585	0.25
G	1.2 × 1.2	2.53/40/2.53	1600	79.860	10.580	2.640	1.020	0.17	0.0585	0.25
H	1.2 × 1.2	3.37/40/3.37	1600	79.860	10.580	2.640	1.020	0.17	0.0585	0.25
I	1.2 × 1.2	3.37/50/3.37	1600	114.580	10.580	2.640	1.020	0.17	0.0590	0.25
K	1.2 × 1.2	3.37/50/3.37	1600	218.140	10.580	2.640	1.020	0.17	0.0595	0.25

The natural frequencies of sixteen above free-free composite sandwich beams were calculated by ANSYS finite element codes. The apparent bending stiffness of the beam is obtained according to the following expression [13]:

$$D_{xn} = 4\pi^2 f_{xn}^2 m^* L_x^4/\alpha_n^4, \quad D_{yn} = 4\pi^2 f_{yn}^2 m^* L_y^4/\alpha_n^4, \tag{30}$$

where f_n is the eigenfrequency for mode n; L is the length and m^* is the mass per unit area. Here, for the beam studied with free-free boundary conditions, the values of α_n can be found in Ref. [13].

The first ten eigenfrequencies and corresponding apparent bending stiffnesses of beams A0, A90, C0 and C90, for example, are shown in Table 2. The apparent bending stiffness curve and function along the entire frequency range of interest are reconstructed by applying the LS method to the set of (f_{xn}, D_{xn}) and (f_{yn}, D_{yn}) points obtained numerically for each eigenfrequency.

Table 2. Eigenfrequencies and apparent bending stiffnesses of four beams

Mode	Beam A0		Beam A90		Beam C0		Beam C90	
	f (Hz)	D_x (Nm)	f (Hz)	D_y (Nm)	f (Hz)	D_x (Nm)	f (Hz)	D_y (Nm)
1	82.334	10523.81	95.643	10026.90	82.076	13779.59	94.927	13014.55
2	223.59	10230.23	256.26	9488.29	216.69	12660.41	237.56	10743.91
3	407.07	8826.87	468.10	8241.22	397.31	11079.41	425.86	8987.47
4	596.87	6944.65	650.30	5820.55	574.29	8471.15	609.77	6743.07
5	675.41	3984.97	726.59	3256.23	646.20	4806.33	689.32	3861.60
6	707.32	2240.37	761.04	1831.25	672.17	2665.84	722.84	2176.74
7	784.18	1553.56	840.93	1261.42	739.37	1819.74	798.40	1498.21
8	855.54	1120.85	920.24	915.62	806.86	1313.56	874.31	1089.01
9	897.52	790.56	970.72	652.95	841.34	915.33	918.13	769.64
10	934.56	574.38	1016.2	479.50	876.75	666.08	962.95	567.32

5. VALIDATION STUDY

For the validation test, the STL across a finite aluminium sandwich plate with poroelastic material is calculated and compared with theoretical result of Bolton et al. [3]. The property parameters of aluminium plates and poroelastic material are presented in Table 3.

It is obvious from Fig. 3 that there is an acceptable agreement between present analytical and theoretical results shown in [3].

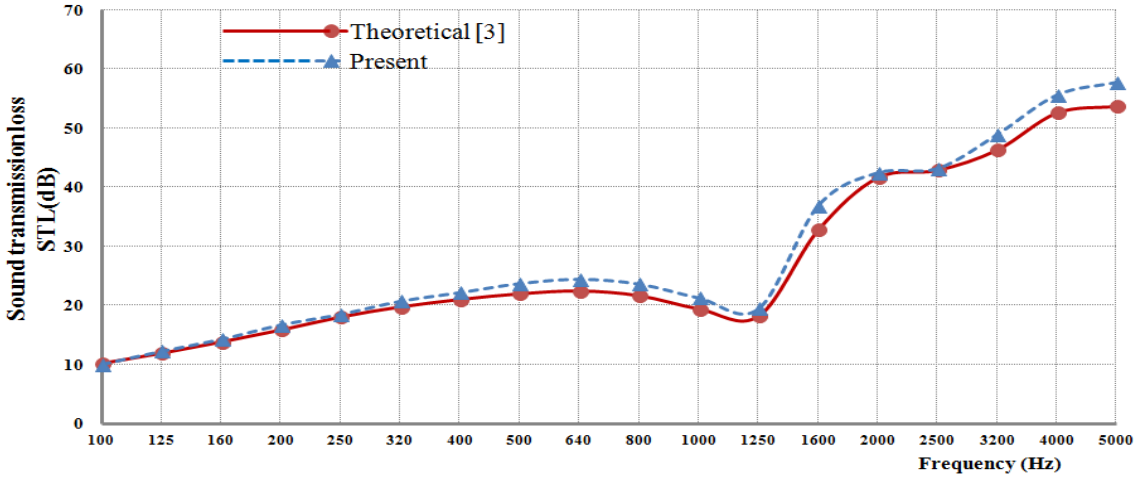

Fig. 3. Comparison of STL between the current study and result of Bolton et al. [3]

Table 3. Parameters of the aluminium skin and the core layer

Parameter	Symbol	Value
The skin of sandwich plate		
Young's Modulus	E_s	70 GPa
Density	ρ_s	2700 kg/m^3
Poisson's ratio	v_s	0.33
Upper plate thickness	h_1	1.27 mm
Bottom plate thickness	h_2	0.762 mm
Length $\times$ Width of plate	$a \times b$	1.2 $\times$ 1.2 m
Porous layer thickness	H	27 mm
Initial amplitude of incident wave	I_0	1 m^2/s
The core of sandwich plate		
Density	ρ_c	30 kg/m^3
Young's Modulus	E_c	8.105 Pa
Poisson's ratio	v_c	0.40

6. EXPERIMENTAL STUDY

The STL of the eight sandwich plates are measured according to ISO 140-4 [21]. The test samples are clamped between two reverberation rooms, one (2.06 m $\times$ 3.7 m $\times$ 2.1 m) is used as the source room and the other (1.54 m $\times$ 3.7 m $\times$ 2.1 m) is the receiving room, as shown in Fig. 4.

Fig. 4. Test arrangement for samples

The sound transmission loss is determined by [21]:

$$STL = L_1 - L_2 + 10 \log \left(\frac{A_P T}{0.161 V_2} \right) \tag{31}$$

where L_1 and L_2 are the average sound pressure levels in the source and receiving room, respectively. A_p is the test-specimen area; V_2 is the volume of the receiving room; T is the reverberation time of the receiving room when the sandwich plate is clamped between the two rooms. The mounting conditions are described in Fig. 4. Eight composite sandwich plates are tested, and together with prediction, the results are shown in Figs. 5–8.

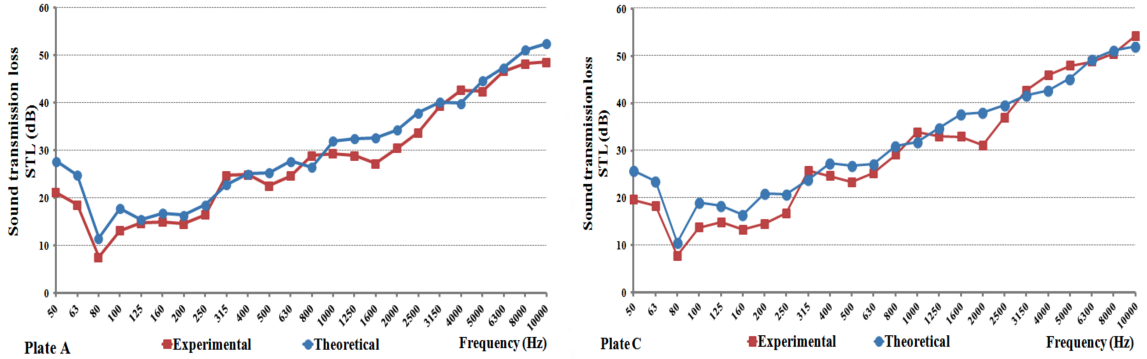

Fig. 5. Measured and predicted STL for Plate A and C

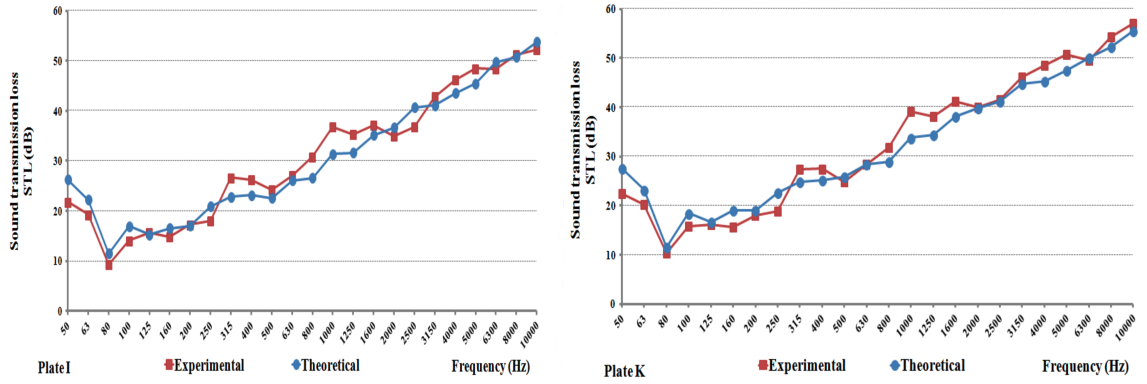

Fig. 6. Measured and predicted STL for Plate I and K

From Fig. 5 to Fig. 8, as can be seen that experimental results approximately agree with the theoretical prediction. As shown, for example, with plate A, at low frequencies, below 200 Hz, the difference between measurement and prediction is less than 6 dB. At frequency 1600 Hz, this difference is 7 dB. The similarity between the measured and the calculated results over the remaining frequency range is observed. Experimental researches have shown that the boundary conditions may have some influences on STL below the coincidence frequency. Secondly, around the coincidence frequency, theoretical results seem to overestimate STL compared with experiments.

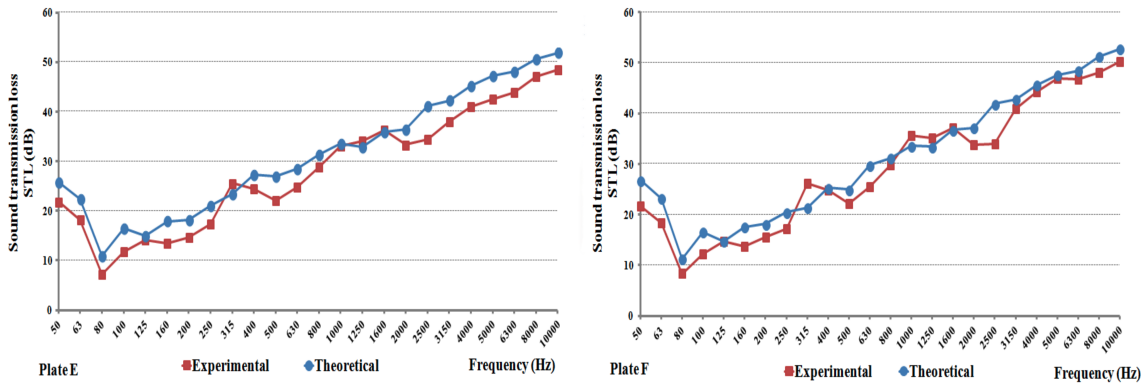

Fig. 7. Measured and predicted STL for Plate E and F

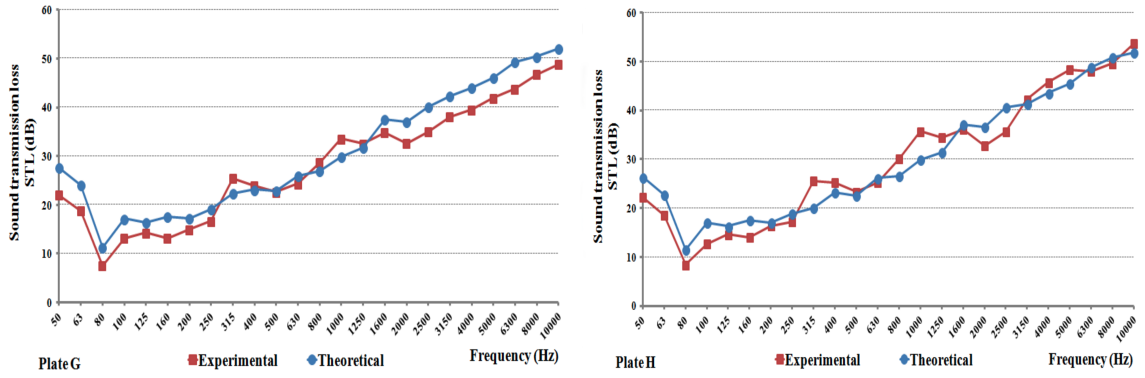

Fig. 8. Measured and predicted STL for Plate G and H

- From Figs. 5 and 6, described the STL across plate A, plate C and plate I, plate K respectively, we can see that, increasing the core density increases considerably the STL through the sandwich plates, specifically for sandwich plate K versus plate I:

+ In the low frequency region ($f < 125$ Hz), theoretically, the STL increases by 1,484 dB at 100 Hz; experimentally, the STL increased by 1.76 dB.

+ In the mid frequency region (125 Hz $< f <$ 2000 Hz), theoretically, the STL increases by 3,206 dB at 2000 Hz; experimentally, the STL increased by 4.97 dB.

+ In the high frequency region ($f >$ 2000 Hz), theoretically, the STL increases by 1,711 dB at 10000 Hz; experimentally, the STL increases by 4.79 dB at this same frequency.

- Figs. 6 and 7 compared the measured and predicted STL for plate G with plate H and plate E with plate F respectively. It is obvious that, the STL through the sandwich plates increases as the thickness of the skin plates increased, for example with plate F (compare to plate E):

+ In the low frequency region ($f < 125$ Hz), theoretically, the STL increases by 0.4 dB at 80 Hz; experimentally, the STL increased by 1.04 dB.

+ In the mid frequency region (125 Hz $< f <$ 2000 Hz), theoretically, the STL increases by 0.3 dB at 1000 Hz; experimentally, the STL increased by 2.49 dB.

+ In the high frequency region ($f > 2000$ Hz), theoretically, the STL increases by 0.3 dB at 5000 Hz; experimentally, the STL increases by 4.4 dB at this same frequency.

7. CONCLUSIONS

In this paper, based on a new approach, the forced vibration equation of the composite sandwich plate with foam core is replaced by the vibration equation of an orthotropic plate with two apparent bending stiffnesses in the two principal directions of the plate. The apparent bending stiffnesses of composite sandwich plate are estimated basing on the natural frequencies calculated by the finite element method for the composite sandwich beams cut from the considered composite sandwich plates (without any costly experiments). Finally, the sound transmission loss through clamped finite rectangular composite sandwich plates with foam core is predicted with modal expansion method.

A series of sound transmission loss measurements were conducted on composite sandwich plates with skin layers of fiberglass/polyester and core layer of porous polyurethane.

Theoretical predictions agree well with the experimental results in most frequency ranges of interest. The theoretical approach presented in this work may provide a simple tool for predicting the STL of finite composite sandwich structures with foam core.

REFERENCES

[1] R. D. Ford, P. Lord, and A. W. Walker. Sound transmission through sandwich constructions. *Journal of Sound and Vibration*, **5**, (1967), pp. 9–21. https://doi.org/10.1016/0022-460x(67)90173-3.

[2] J. A. Moore and R. H. Lyon. Sound transmission loss characteristics of sandwich panel constructions. *The Journal of the Acoustical Society of America*, **89**, (1991), pp. 777–791. https://doi.org/10.1121/1.1894638.

[3] J. S. Bolton, N.-M. Shiau, and Y. J. Kang. Sound transmission through multi-panel structures lined with elastic porous materials. *Journal of Sound and Vibration*, **191**, (1996), pp. 317–347. https://doi.org/10.1006/jsvi.1996.0125.

[4] R. Cherif and N. Atalla. Experimental investigation of the accuracy of a vibroacoustic model for sandwich-composite panels. *The Journal of the Acoustical Society of America*, **137**, (2015), pp. 1541–1550. https://doi.org/10.1121/1.4908239.

[5] S. Hwang, J. Kim, S. Lee, and H. Kwun. Prediction of sound reduction index of double sandwich panel. *Applied Acoustics*, **93**, (2015), pp. 44–50. https://doi.org/10.1016/j.apacoust.2015.01.017.

[6] K. C. Sahu, J. Tuhkuri, and J. N. Reddy. Active attenuation of sound transmission through a soft-core sandwich panel into an acoustic enclosure using volume velocity cancellation. *Proceedings of the Institution of Mechanical Engineers, Part C: Journal of Mechanical Engineering Science*, **229**, (2015), pp. 3096–3112. https://doi.org/10.1177/0954406215569896.

[7] V. D'Alessandro, G. Petrone, F. Franco, and S. D. Rosa. A review of the vibroacoustics of sandwich panels: Models and experiments. *Journal of Sandwich Structures & Materials*, **15**, (2013), pp. 541–582. https://doi.org/10.1177/1099636213490588.

[8] C. Shen, F. X. Xin, and T. J. Lu. Theoretical model for sound transmission through finite sandwich structures with corrugated core. *International Journal of Non-Linear Mechanics*, **47**, (2012), pp. 1066–1072. https://doi.org/10.1016/j.ijnonlinmec.2011.09.014.

[9] C. J. Naify, C. Huang, M. Sneddon, and S. Nutt. Transmission loss of honeycomb sandwich structures with attached gas layers. *Applied Acoustics*, **72**, (2011), pp. 71–77. https://doi.org/10.1016/j.apacoust.2010.09.005.

[10] R. D. Mindlin. Influence of rotatory inertia and shear on flexural motions of isotropic, elastic plates. *Journal of Applied Mechanics*, **18**, (1951), pp. 31–38. https://doi.org/10.1115/1.4010217.

[11] W. Shengchun, D. Zhaoxiang, and S. Weidong. Sound transmission loss characteristics of unbounded orthotropic sandwich panels in bending vibration considering transverse shear deformation. *Composite Structures*, **92**, (2010), pp. 2885–2889. https://doi.org/10.1016/j.compstruct.2010.04.014.

[12] J. Zhou, A. Bhaskar, and X. Zhang. Sound transmission through a double-panel construction lined with poroelastic material in the presence of mean flow. *Journal of Sound and Vibration*, **332**, (2013), pp. 3724–3734. https://doi.org/10.1016/j.jsv.2013.02.020.

[13] E. Nilsson and A. C. Nilsson. Prediction and measurement of some dynamic properties of sandwich structures with honeycomb and foam cores. *Journal of Sound and Vibration*, **251**, (2002), pp. 409–430. https://doi.org/10.1006/jsvi.2001.4007.

[14] Y. Qu, Z. Peng, W. Zhang, and G. Meng. Nonlinear vibro-acoustic behaviors of coupled sandwich cylindrical shell and spring-mass-damper systems. *Mechanical Systems and Signal Processing*, **124**, (2019), pp. 254–274. https://doi.org/10.1016/j.ymssp.2019.01.048.

[15] B. R. Mace and E. Manconi. Modelling wave propagation in two-dimensional structures using finite element analysis. *Journal of Sound and Vibration*, **318**, (2008), pp. 884–902. https://doi.org/10.1016/j.jsv.2008.04.039.

[16] C. Droz, C. Zhou, M. N. Ichchou, and J.-P. Lainé. A hybrid wave-mode formulation for the vibro-acoustic analysis of 2D periodic structures. *Journal of Sound and Vibration*, **363**, (2016), pp. 285–302. https://doi.org/10.1016/j.jsv.2015.11.003.

[17] D. Chronopoulos, M. Ichchou, B. Troclet, and O. Bareille. Computing the broadband vibroacoustic response of arbitrarily thick layered panels by a wave finite element approach. *Applied Acoustics*, **77**, (2014), pp. 89–98. https://doi.org/10.1016/j.apacoust.2013.10.002.

[18] Y. Yang, B. R. Mace, and M. J. Kingan. Prediction of sound transmission through, and radiation from, panels using a wave and finite element method. *The Journal of the Acoustical Society of America*, **141**, (2017), pp. 2452–2460. https://doi.org/10.1121/1.4977925.

[19] Y. Yang, B. R. Mace, and M. J. Kingan. Wave and finite element method for predicting sound transmission through finite multi-layered structures with fluid layers. *Computers & Structures*, **204**, (2018), pp. 20–30. https://doi.org/10.1016/j.compstruc.2018.04.003.

[20] T. J. Lu and F. X. Xin. *Vibro-acoustics of lightweight sandwich*. Science Press Beijing and Springer-Verlag Berlin Heidenberg, (2014).

[21] ISO 140-4. *Acoustics - Measurement of sound insulation in buildings and of building elements - Part 4: Field measurements of airborne sound insulation between rooms*. (1998).